EGU2020: Sharing Geoscience Online

Was the 2019 Ms6.0 Changning Earthquake in Sichuan, China caused by Human Activities?

—— Analysis of the Fault Structure and Seismogenic Mechanism based on InSAR

Authors: Gao Hua; Liao Mingsheng; Xu Wenbin; Liu Xiaoge

武漢大學 WUHAN UNIVERSITY LIESMARS

Wuhan University
State Key Laboratory of Information Engineering in Surveying, Mapping and Remote Sensing

May, 2020

Content

1 Background

LIESMARS

(1) Background

- On the night of June 17, 2019 (Beijing time), a Ms6.0 earthquake struck Changning county of Sichuan province where is one of China‘s important shale gas reservoirs.
- 5023 aftershocks, including 4 Ms>5 events.
- Before this, there were also one Ms5.7 and one Ms5.3 earthquake in the region.
- 13 people were killed and more than 200 people were injured.
- There are some shale gas wells and injection wells for salt mining around the earthquake area.

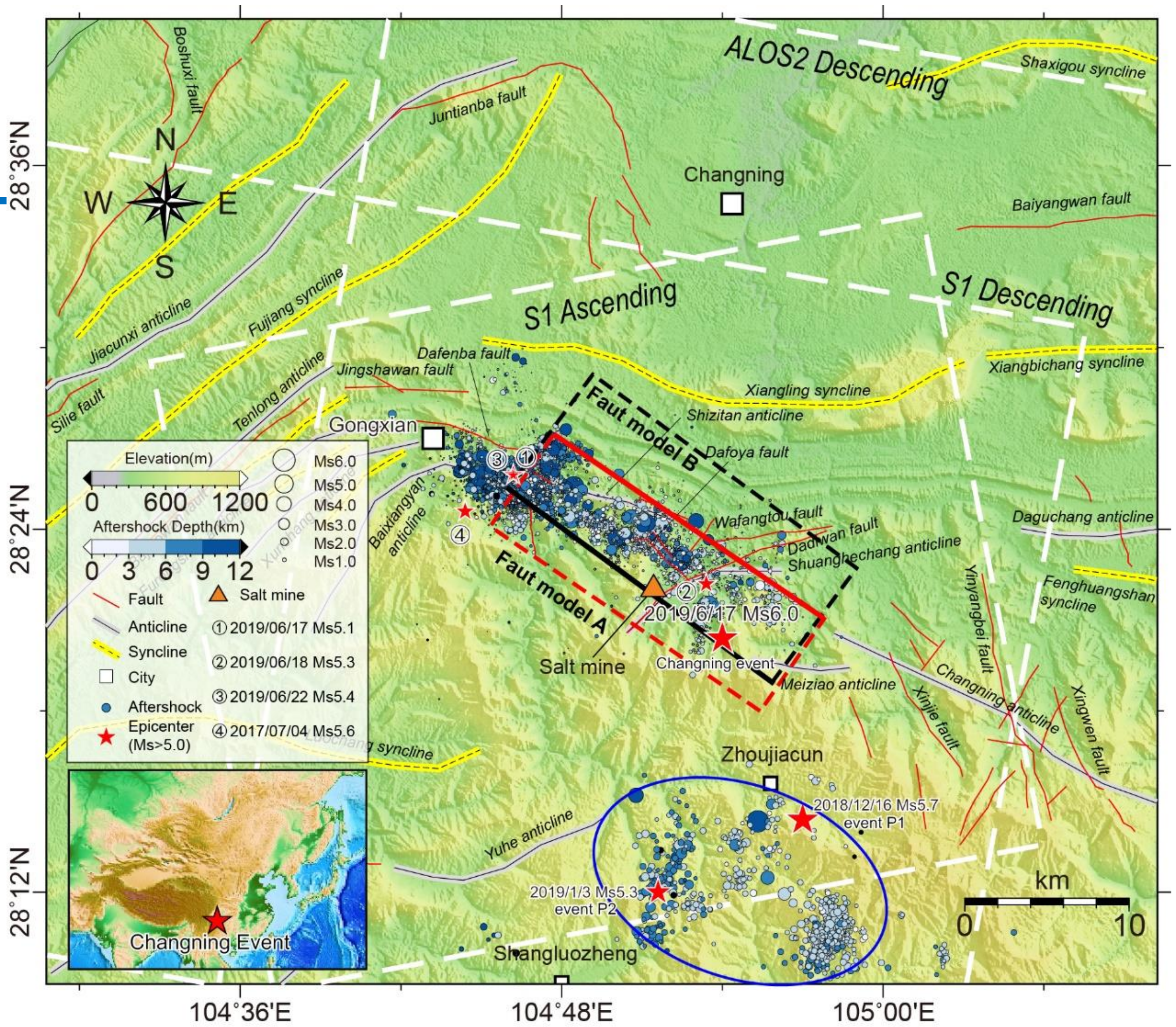

Fig. 1-1 Geotectonic background and aftershocks distribution of the study area. White dotted frames denote the SAR data coverage. Red stars are the epicenters of Ms > 5 earthquakes from 2018/12/16 to 2019/7/4 (CENC). Blue dots denote aftershocks, and those in the middle of the figure are the aftershocks of the Changning event (Yang et al., 2020) and those inside the blue ellipse are of P1 and P2 (Lei et al., 2019a). Orange triangle indicates the salt mine near the epicenter (Ruan et al., 2008). Red and black frames are the surface projection of the fault models. The faults and folds in the map are revised from Yi et al. (2019) and the geological report of the Junlian region.

(1) Background

We want to know that:

Coseismic:

① the area affected by Changning earthquake
② surface deformation
③ the geometry and motion model of the fault

Pre-earthquake:

① what role did two Ms>5.0 earthquakes in this area play before the Changning?
② triggering effect?

After the earthquakes:

① distribution characteristics of aftershocks

cause of the Changning earthquake

2 Co-seismic deformation

(2) Co-seismic deformation

Earthquake time and data coverage time

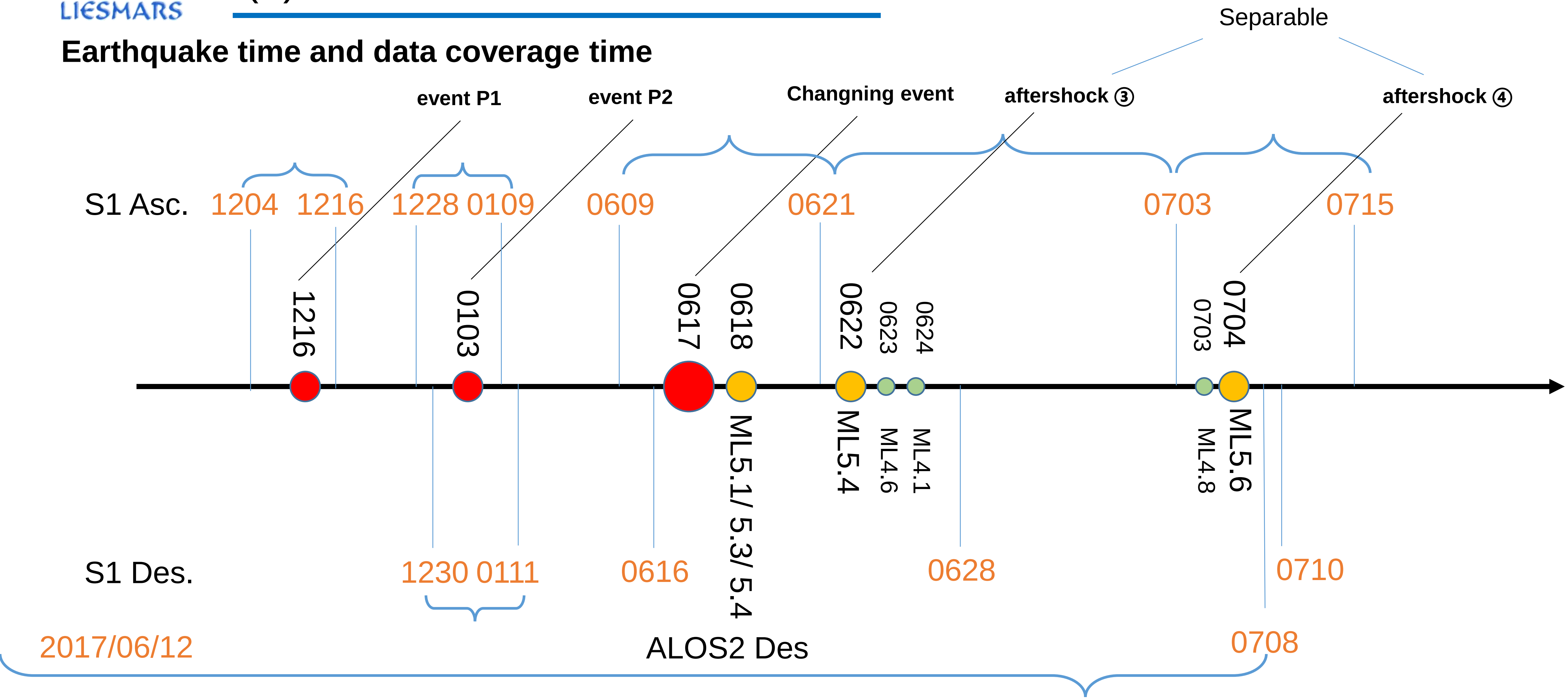

Fig. 2-1 Image information of co-seismic deformation fields

(2) Co-seismic deformation

Table 2-1. Image information processed by D-InSAR

Event	Date yyyymmdd	Satellite	Model	Master yyyymmdd	Slaver yyyymmdd	Baseline (m)	Pass
P1	20181216	Sentinel-1	Asc	20181204	20181216	15	55
			Des	20181206	20181218	162	164
P2	20190103		Asc	20181228	20190109	123	55
			Des	20181230	20190111	9	164
Changning	20190617		Asc	20190609	20190621	29	55
			Des	20190616	20190628	29	164
Aftershock ③	20190622		Asc	20190621	20190703	21	55
Aftershock ④	20190704		Asc	20190703	20190715	28	55
All events	/	ALOS2	Des	20170612	20190708	69	190708

(2) Co-seismic deformation

toward satellite
(positive, **warm color**)

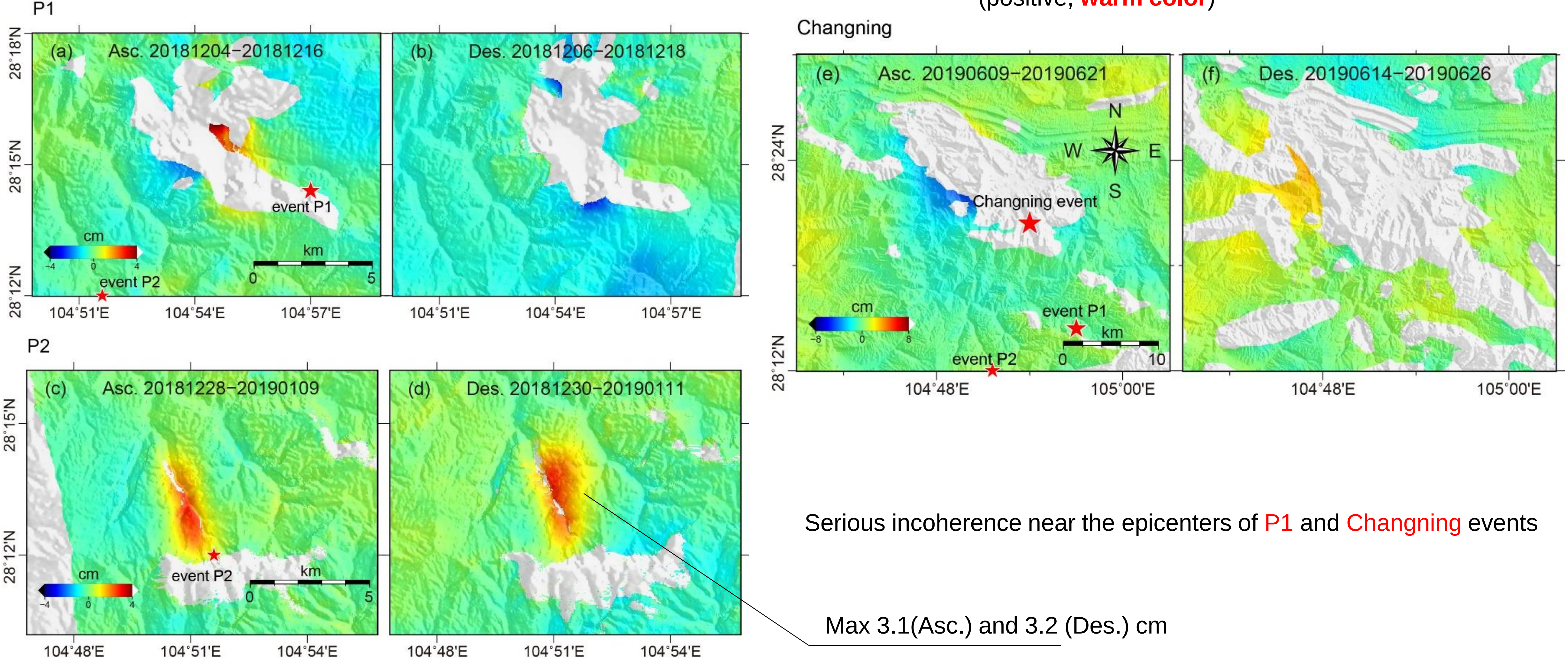

Serious incoherence near the epicenters of P1 and Changning events

Max 3.1(Asc.) and 3.2 (Des.) cm

Fig. 2-2 Coseismic deformation fields of P1, P2 and Changning events obtained by Sentinel-1

(2) Co-seismic deformation

Although the time baseline is up to 756 days, the coseismic deformation results of ALOS2 can clearly distinguish the deformation regions caused P1, P2, and the Changning events.

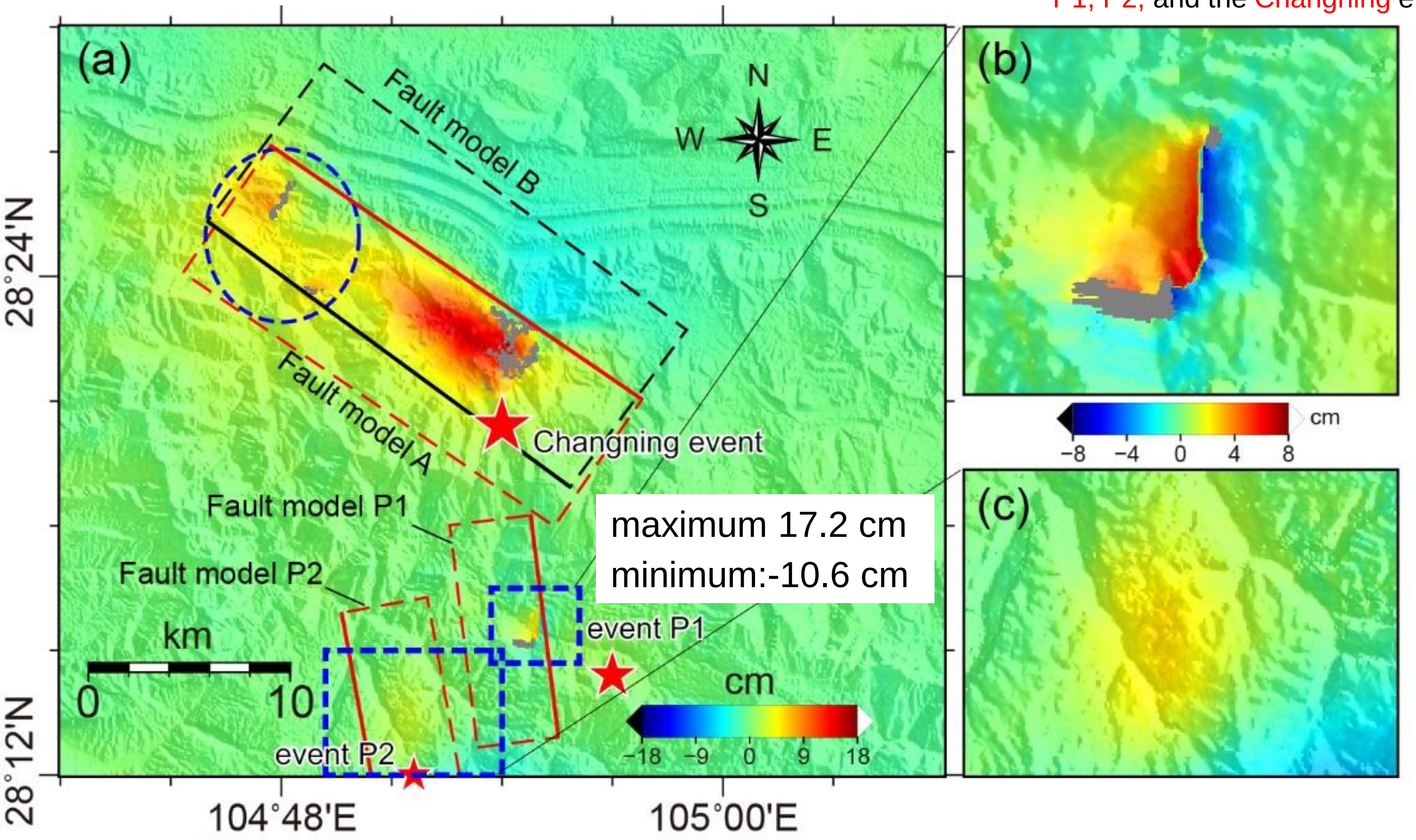

toward satellite
(positive, **warm color**)

maximum: 9.0 cm
minimum: -5.6 cm

maximum: 4.7 cm

Fig. 2-3 The co-seismic deformation of the Changning event, event P1, P2 and aftershocks obtained by ALOS2

(2) Co-seismic deformation

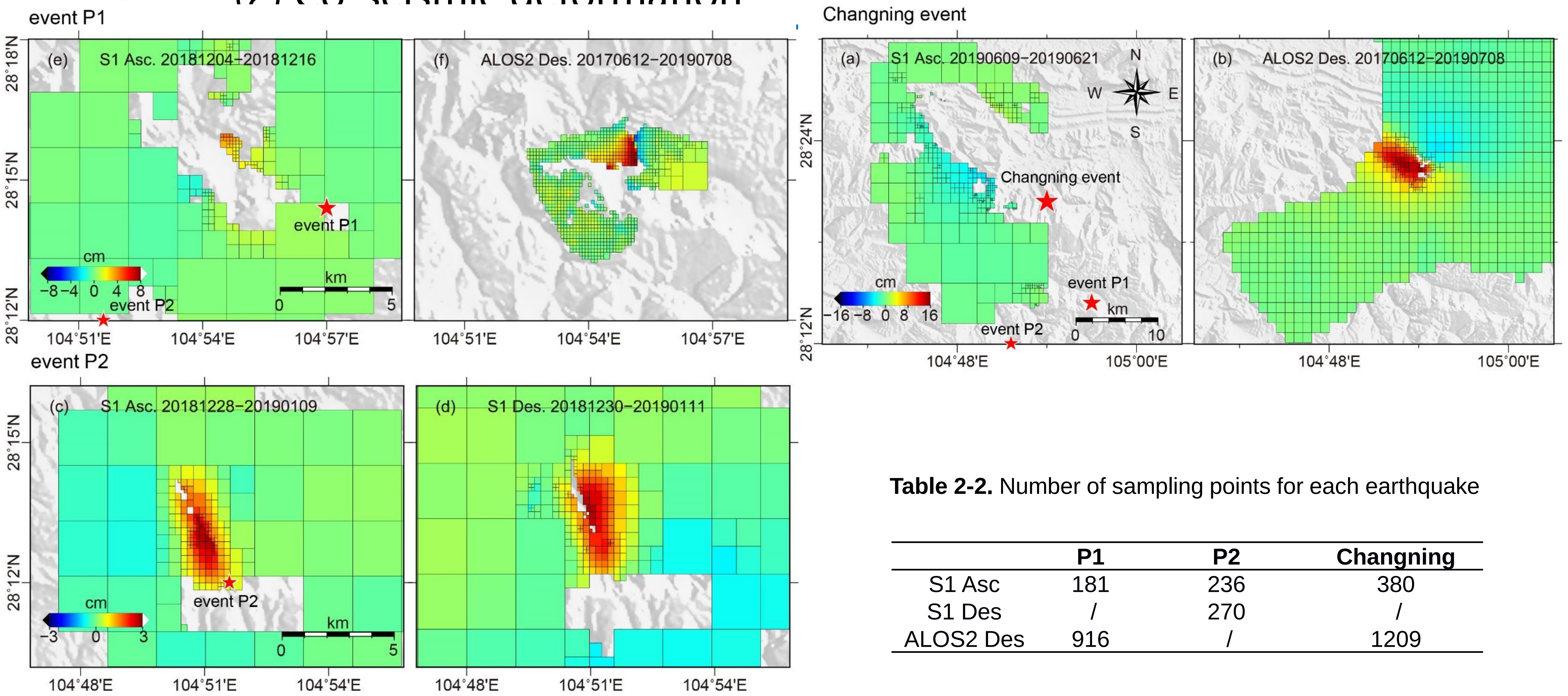

Table 2-2. Number of sampling points for each earthquake

	P1	P2	Changning
S1 Asc	181	236	380
S1 Des	/	270	/
ALOS2 Des	916	/	1209

Fig. 2-4 The deformation points participating in inversion after quad-tree sampling

3 Fault model

(3) Fault model

Table 3-1 The fault parameters of Changning, P1 and P2 from different sources

event	source	lon. /°	lat. /°	depth/km	strike/°	dip/°	rake/°	Mw	Note
Changning	Fault Model A*	104.855	28.375	4.6	125	50	38	5.72	rms(0.82cm)
	Fault Model B*	104.875	28.400	4.1	306	43	75	5.82	rms(0.87cm)
	Yi et al., 2019	104.905	28.344	3	131	51	36	5.79	Plane 1
	Guo., 2019	/	/	15.5	151	45	77	5.76	Plane 1
	CENC	104.900	28.340	16	/	/	/	/	/
	USGS	104.857	28.405	11.5	308	45	40	5.79	Plane 1
	GCMT	104.960	28.360	12	323	57	65	5.7	Plane 1
P1	This study*	104.901	28.258	1.7	172	44	53	4.63	rms(0.80cm)
	Yi et al., 2019	104.948	28.219	3	349	76	-5	5.17	Plane 2
	CENC	104.950	28.240	12	/	/	/	/	/
	USGS	105.013	28.295	18.6	349	83	-3	5.28	Plane 2
	GCMT	105.090	28.200	14	348	84	-9	5.3	
P2	This study*	104.856	28.224	2.3	349	50	87	4.81	rms(0.32cm)
	Yi et al., 2019	104.861	28.192	2	351	46	46	4.81	Plane 2
	CENC	104.860	28.200	15	/	/	/	/	/
	USGS	104.918	28.190	11.5	355	48	59	4.85	Plane 2
	GCMT	104.950	28.210	12	349	41	43	5	/

* The parameters obtained in this paper are the results of non-linear inversion. The epicenter parameters (including longitude, latitude and depth) are all the geometric centers of faults.

(3) Fault model

Table 3-1 The fault parameters of Changning, P1 and P2 from different sources

event	source	lon. /°	lat. /°	depth/km	strike/°	dip/°	rake/°	Mw	Note
Changning	Fault Model A*	104.855	28.375	4.6	125	50	38	5.72	rms(0.82cm)
	Fault Model B*	104.875	28.400	4.1	306	43	75	5.82	rms(0.87cm)
	Yi et al., 2019	104.905	28.344	3	131	51			
	Guo., 2019	/	/	15.5	151	45			
	CENC	104.900	28.340	16	/	/			
	USGS	104.857	28.405	11.5	308	45			
	GCMT	104.960	28.360	12	323	57			
P1	This study*	104.901	28.258	1.7	172	44			
	Yi et al., 2019	104.948	28.219	3	349	76			
	CENC	104.950	28.240	12	/	/			
	USGS	105.013	28.295	18.6	349	83			
	GCMT	105.090	28.200	14	348	84			
P2	This study*	104.856	28.224	2.3	349	50			
	Yi et al., 2019	104.861	28.192	2	351	46			
	CENC	104.860	28.200	15	/	/			
	USGS	104.918	28.190	11.5	355	48			
	GCMT	104.950	28.210	12	349	41			

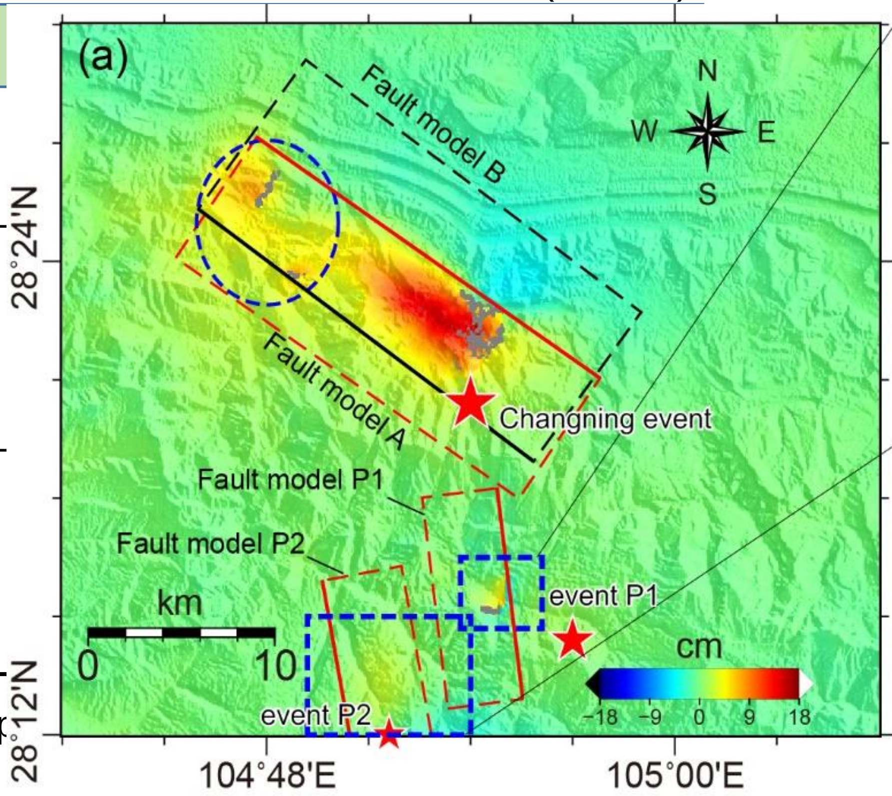

* The parameters obtained in this paper are the results of non-linear inversion. The epicenter p
and depth) are all the geometric centers of faults.

(3) Fault model

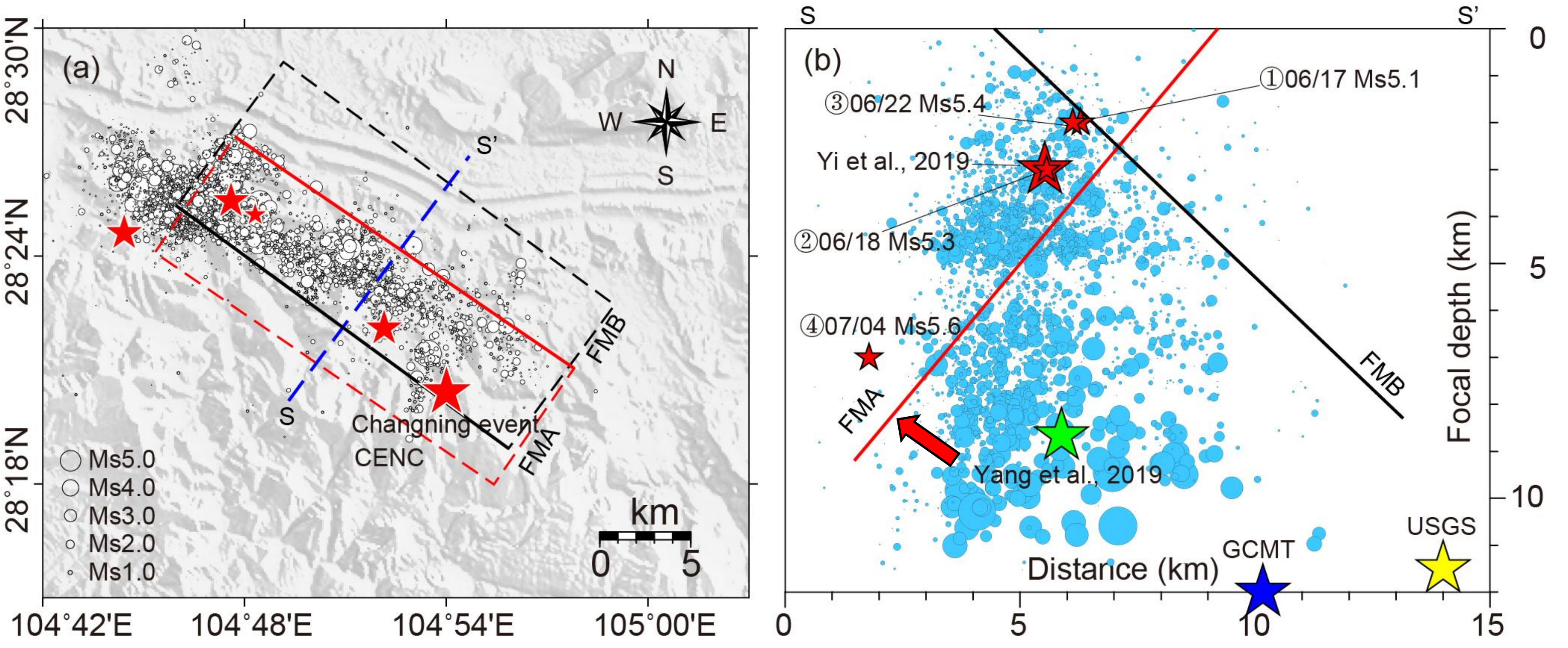

Fig. 3-1 Aftershock distribution and profile

Figure a shows the distribution of aftershocks and the surface projection of FMA and FMB. Figure b shows the section of the blue dotted line in Figure a. The green stars in Figure b are the main and aftershock epicenters relocated by Yi et al. (2019).

FMA is more consistent with the aftershock distribution obtained by aftershock relocation. According to FMB, most aftershocks occurred in the footwall and few occurred in the hanging wall. This is inconsistent with the spatial distribution pattern of aftershocks and fault.

(3) Fault model

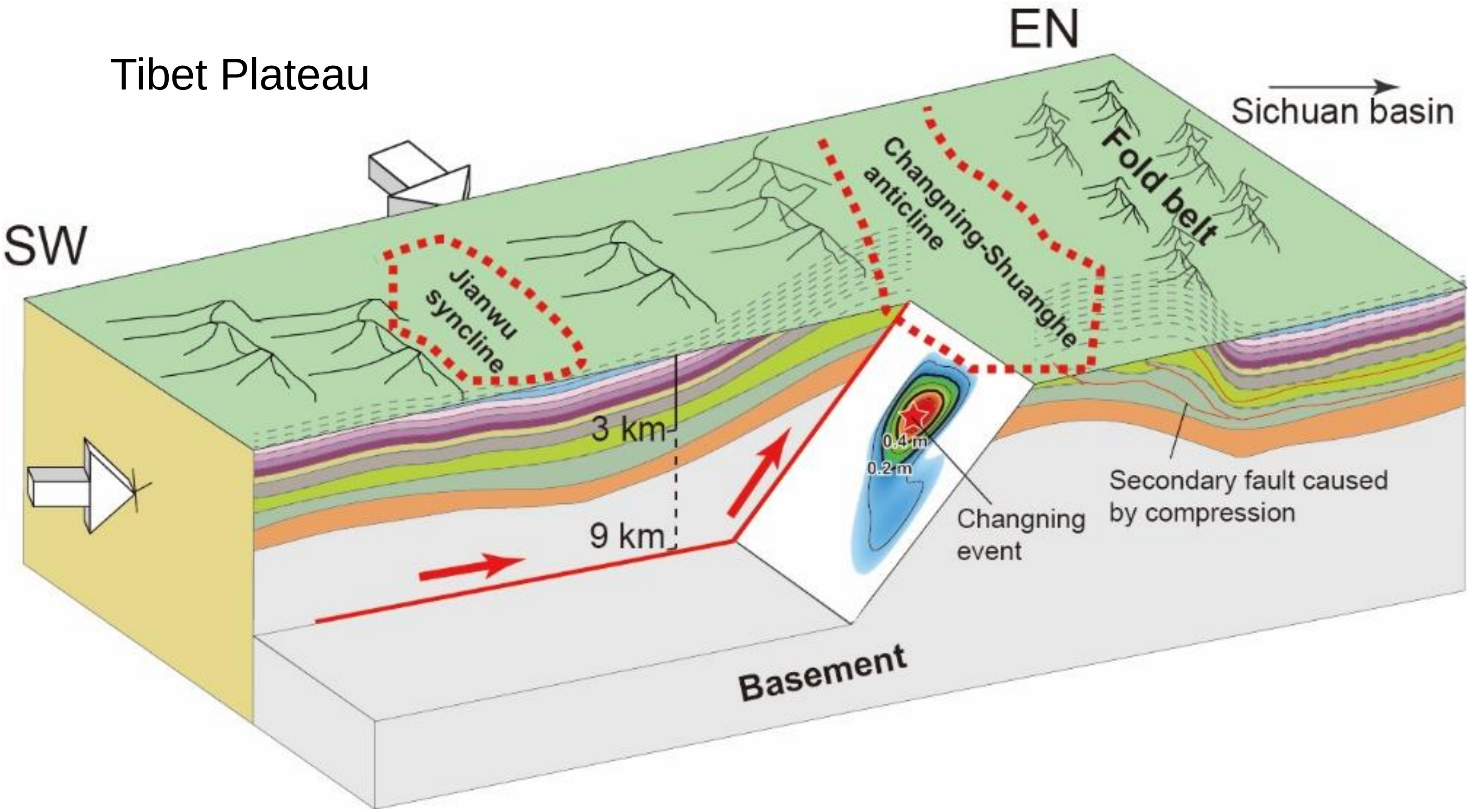

The result of seismic reflection profile analysis shows that there may be a fault inclining southwest in the basement of the south wing, which produces shear slip under tectonic compression in the southwest (He et al., 2019).

Fig. 3-2 Cartoon of stratigraphic and fault structure in the Changning area. The slope on the white background is a contour map of FMA. The red star is the largest slip in the Changning event. The fine red line is the secondary fault and the thick red line is the inferred basement fault. The white arrow denotes the direction of extrusion or material transfer.

(3) Fault model

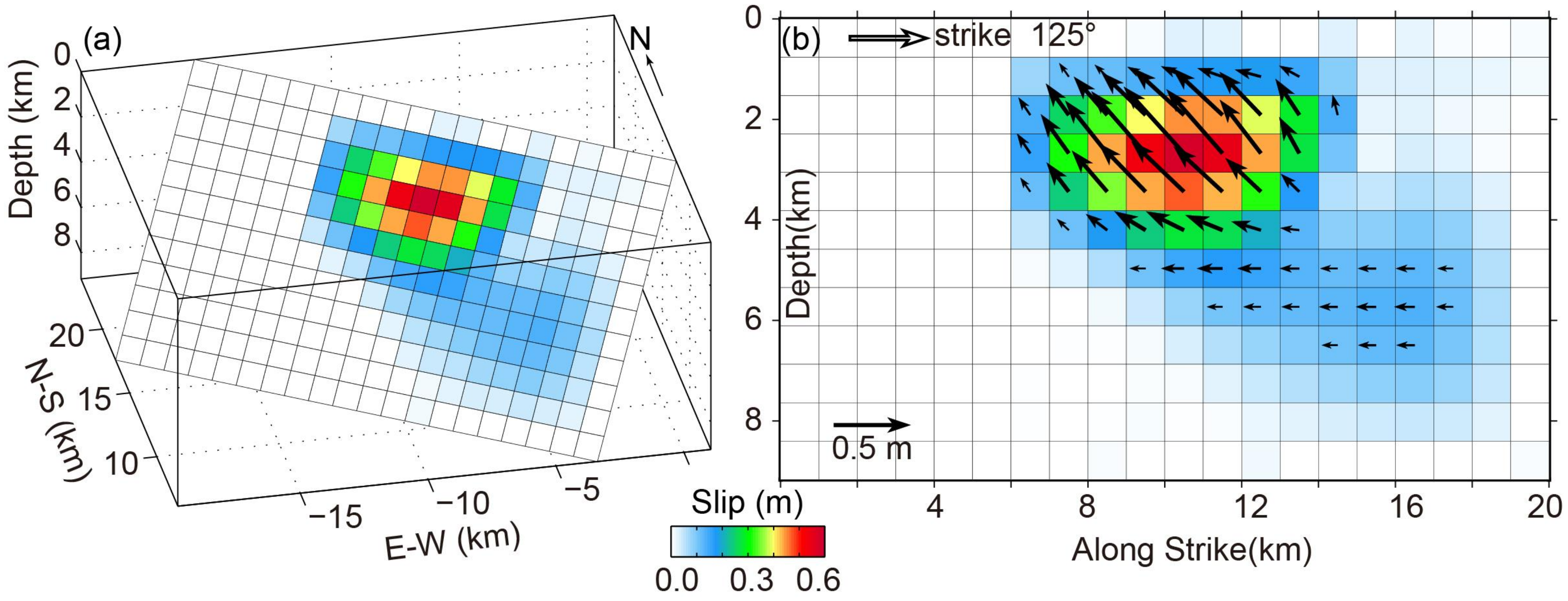

Fig. 3-3 The 3D and 2D model of fault slip distribution of the Changning event

Each small rectangle in the figures represents a slip unit, and the color of the rectangle represents the slip value.

max slip: 0.58 m
3 km depth

Mo: 4.79×10^{17} Nm

Mw: 5.754

the Changning event is caused by a **thrust** slip of a northwest strike fault accompanied by some component of **left-lateral** slip

4 Cause analysis of the Changning earthquake

(4) Cause analysis of the Changning earthquake

- Cause of the Changning event
  - Natural
    - Tectonic movement
    - Pre-earthquake triggering
  - Human induced
    - Hydraulic fracturing
    - Water injection (water volume change)

(4) Cause analysis of the Changning earthquake

Cause of the Changning event

- Natural
  - Tectonic movement √ → 4.4
  - Pre-earthquake triggering × → 4.1
- Human induced
  - Hydraulic fracturing × → 4.2
  - Water injection (water volume change) × → 4.3

(4) Cause analysis of the Changning earthquake

4.1 Pre-earthquake triggering?

maximum 0.006 MPa

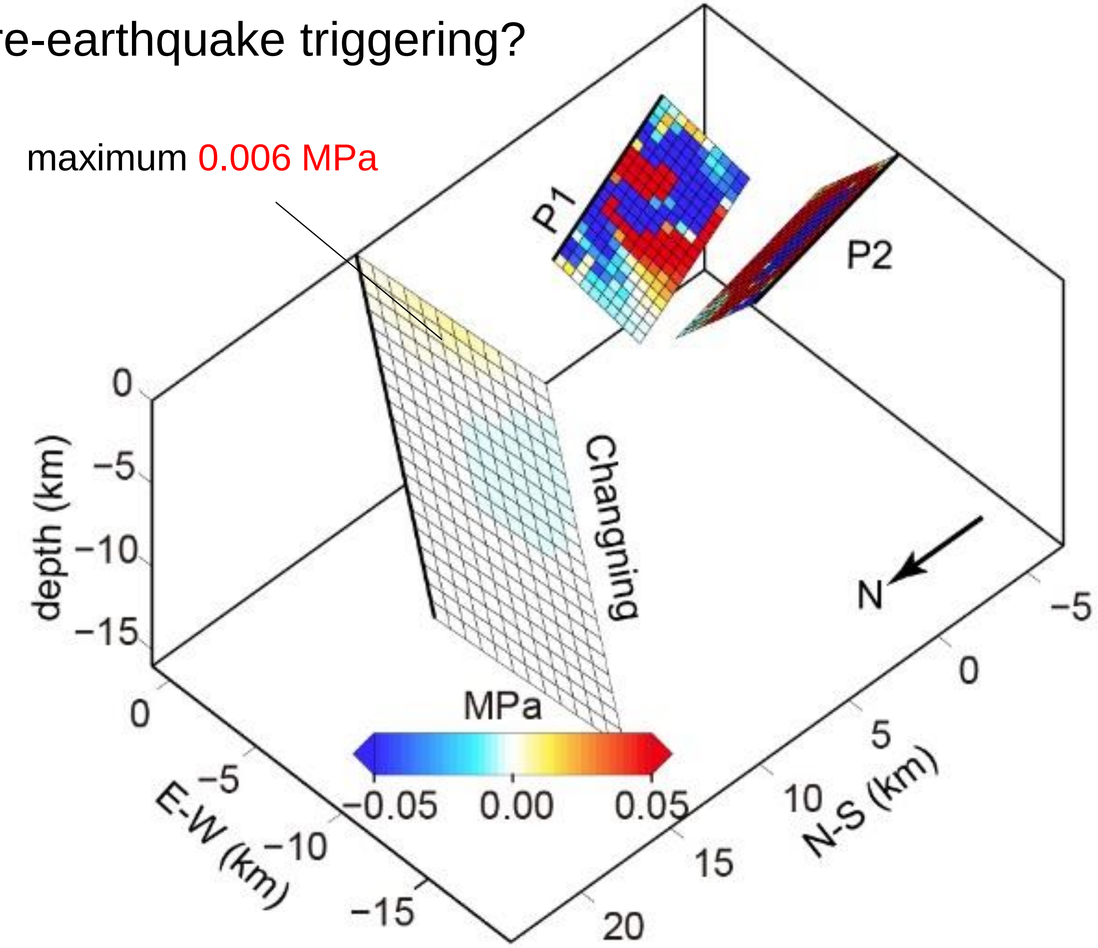

Fig. 4-1 The Coulomb stress change after P1 and P2
Figure a shows the stress changes on the causative fault of the Changning event after event P1 and P2.

The stress change on the causative fault is very little, with the maximum and minimum of 0.006 MPa and -0.003 MPa, respectively. This stress change is too small to trigger an Ms 6.0 earthquake. Generally, the stress threshold should be above 0.01 MPa for triggering an earthquake (Lockner & Beeler., 1999).

(4) Cause analysis of the

4.2 Hydraulic fracturing?

Most of the shale gas wells in Changning area are located **14 km** south of the epicenter of the Changning earthquake (Lei et al., 2019a) with the Meiziao syncline lying between them. The affecting areas of the seismic activity induced by HF or water injection usually within **10 km** of the operation site (Bao & Eaton, 2016; Schultz et al., 2018).

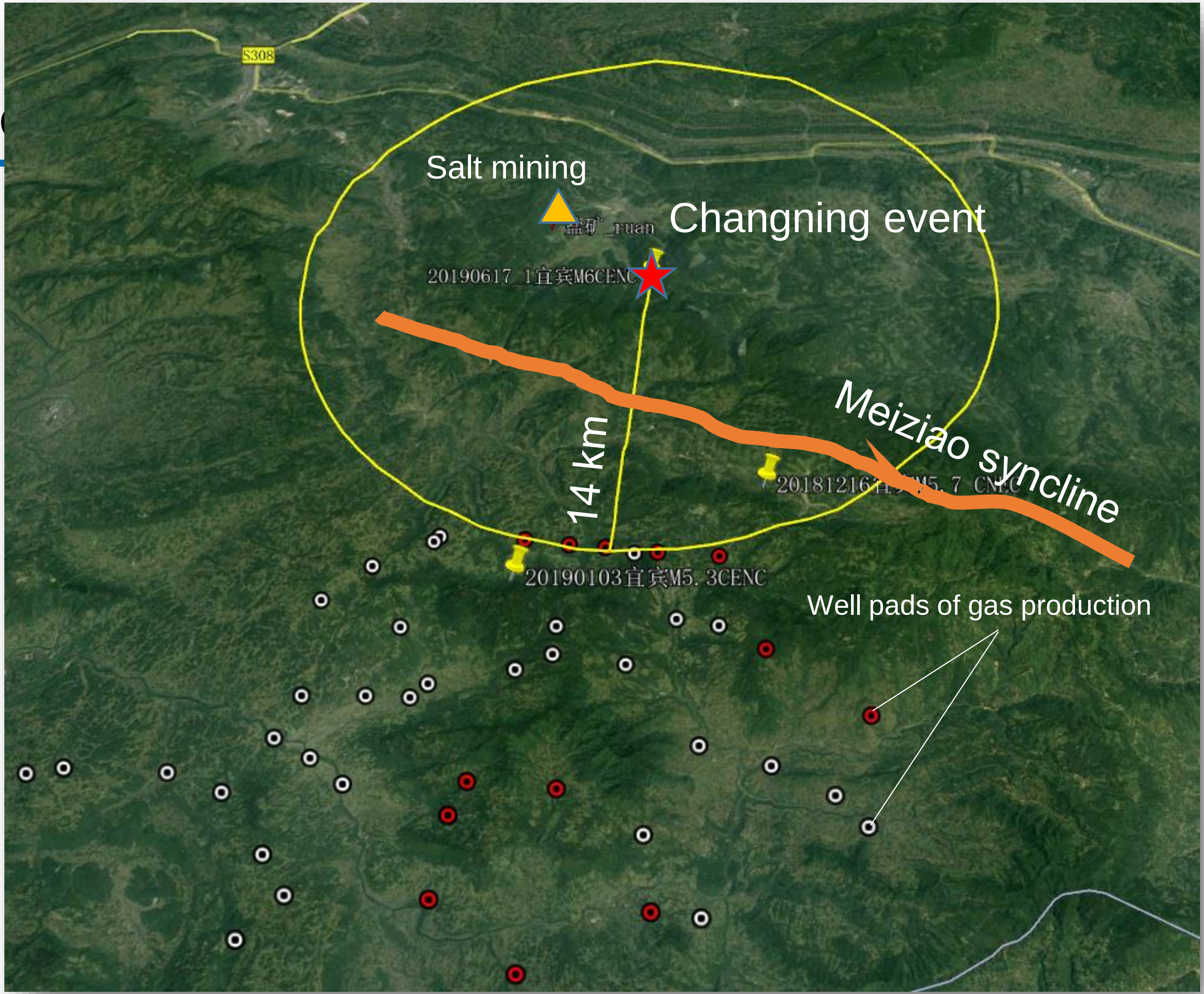

Fig.4-2 The location of Changning earthquake and the near shale gas wells. Background image from Google earth.

(4) Cause analysis of the Changning earthquake

4.3 Water injection (water volume change) ?

$$M_0(\max) = G\Delta V$$ (McGarr, 2014)

- $M_0(\max)$: the **maximum** seismic moment that may be caused by water volume change
- G: shear modulus which is set as 30GPa
- ΔV: water change volume

1.62×10^{6} m^3 ΔV → 4.86×10^{16} Nm, corresponding to *M*w5.1

1.60×10^{7} m^3 ΔV → 4.80×10^{17} Nm, corresponding to *M*w5.75

Tenfold difference

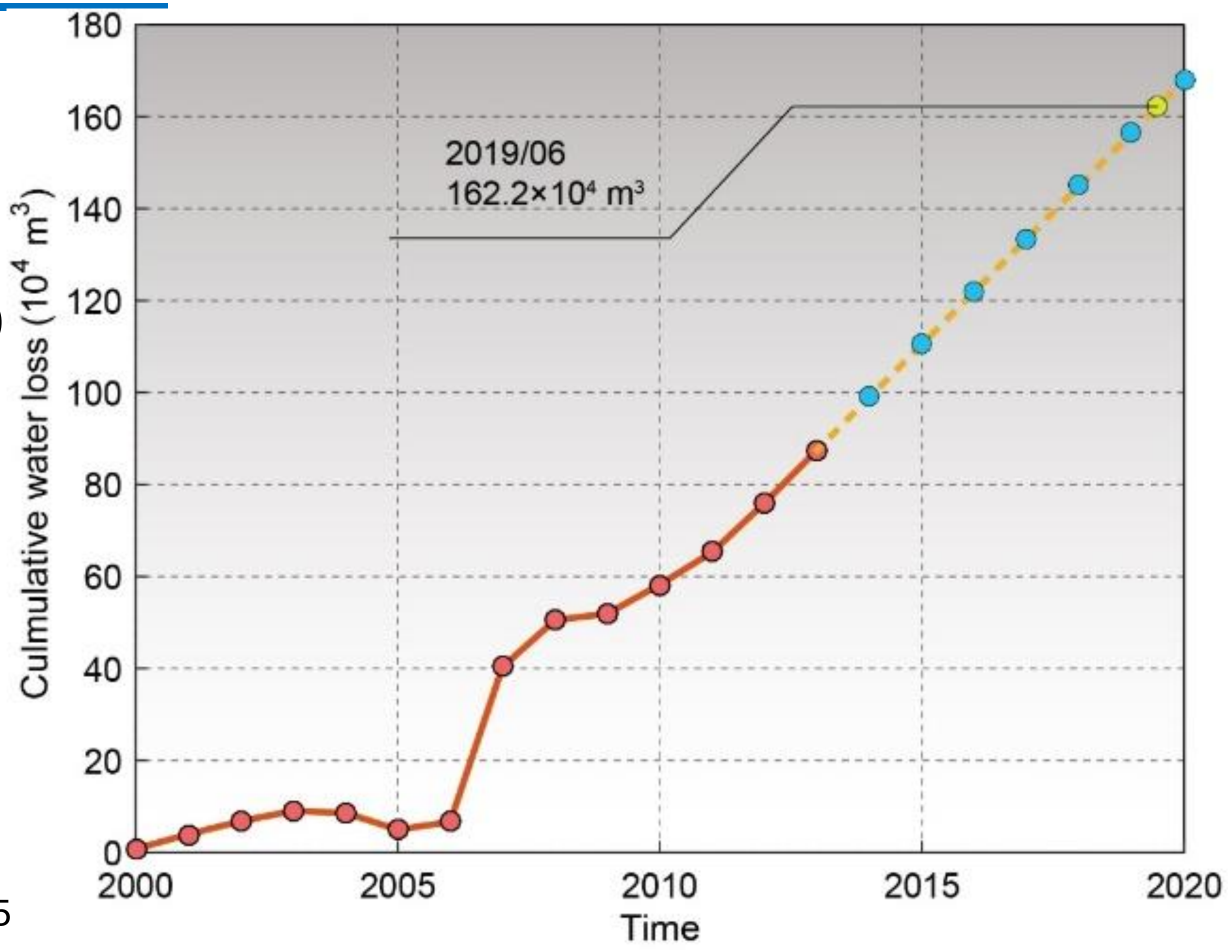

Fig. 4-3. The accumulated water loss of salt mines in 2000-2013 (Sun et al., 2017) and the expected loss in 2014-2020. The loss volume in 2014 and later is calculated according to the loss rate in 2013

(4) Cause analysis of the Changning earthquake

4.4 Tectonic movement

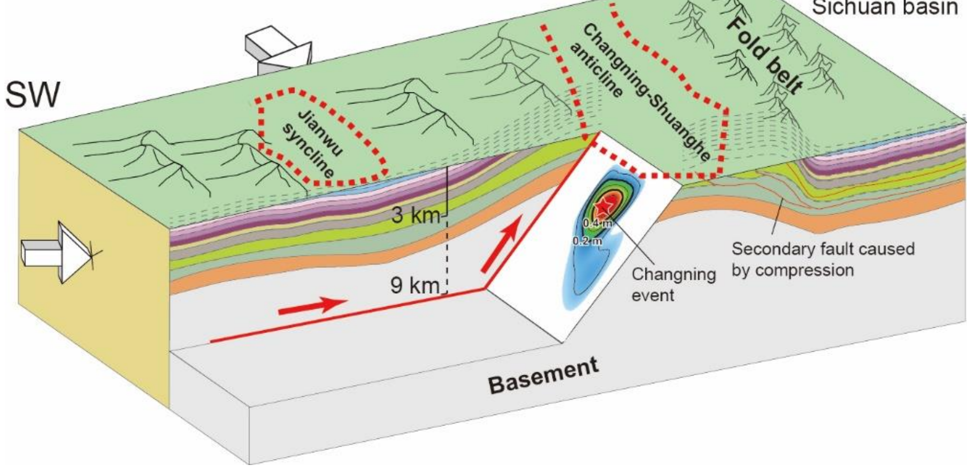

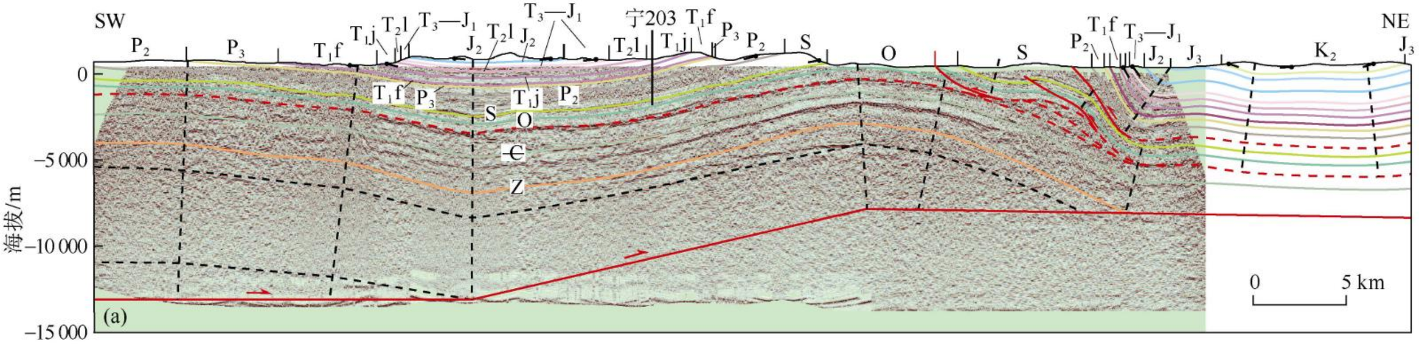

Fig. 4-4 Structural interpretation of seismic reflection profile in the epicenter of the 5.7-magnitude earthquake in Xingwen (P1) (He et al., 2019)

The Changning anticline is **pushed from northwest to southeast**. In addition, because of the obstruction of the basin and its surrounding structures, the area also has **some reverse slip characteristics**. This assumption is confirmed by the tectonic movement characteristics.

5 Conclusion

(5) Conclusion

Co-seismic deformation	• The Changning earthquake caused a deformation area of about 150 km^2 with a maximum of 17.2 cm (LOS) in the northwest of the epicenter.
Fault model	• The FMA, which inclined to the southwest, is more likely to be the fault model of the Changning earthquake. • The event is caused by a thrust slip of a northwest strike fault accompanied by some component of left-lateral slip. • The seismic moment obtained by linear inversion is 4.79×10^{17} Nm corresponding to Mw 5.75.
Cause analysis of the Changning earthquake	• There is no direct relationship between the Changning event and P1 and P2, and we do not find any direct evidence that the Changning event is an induced or triggered earthquake. • We consider that the Changning event is a natural tectonic earthquake.

Reference

Bao, X., & Eaton, D. W. (2016). Fault activation by hydraulic fracturing in western Canada. Science, 354(6318), 1406-1409. http://dx.doi.org/10.1126/science.aag2583

Guo Z. (2019). Moment tensor of Changning Ms6.0 earthquake on June 17, 2019. Retrieved from: http://www.eq-igl.ac.cn/upload/images/2019/6/3d5ec143c5b78d0d.jpg, Accessed date: October 2019.

He, D. F., Lu, R. Q., Huang, H. Y., Wang, X. S., Jiang, H., & Zhang, W. K. (2019). Tectonic and geological setting of the earthquake hazards in the Changning shale gas development zone, Sichuan Basin, SW China. Petroleum Exploration and Development, 46(5), 1051-1064. https://doi.org/10.1016/S1876-3804(19)60262-4

Lei, X., Huang, D., Su, J., Jiang, G., Wang, X., Wang, H., ... & Fu, H. (2017). Fault reactivation and earthquakes with magnitudes of up to Mw4. 7 induced by shale-gas hydraulic fracturing in Sichuan Basin, China. Scientific Reports, 7(1), 1-12. https://doi.org/10.1038/s41598-017-08557-y

Lei, X., Wang, Z., & Su, J. (2019a). The December 2018 ML 5.7 and January 2019 ML 5.3 earthquakes in South Sichuan basin induced by shale gas hydraulic fracturing. Seismological Research Letters, 90(3), 1099-1110. https://doi.org/10.1785/0220190029

Lockner, D. A., & Beeler, N. M. (1999). Premonitory slip and tidal triggering of earthquakes. Journal of Geophysical Research: Solid Earth, 104(B9), 20133-20151. https://doi.org/10.1029/1999JB900205

Maxwell, S. & Norton, M. (2012). Enhancing shale gas reservoir characterization using hydraulic fracture microseismic data. first break 30, 95–101.

McGarr, A. (2014). Maximum magnitude earthquakes induced by fluid injection. Journal of Geophysical Research: solid earth, 119(2), 1008-1019. https://doi.org/10.1002/2013JB010597

Ruan, X., Cheng, W. Z., Zhang, Y. J., Li, J., & Chen, Y. (2008). Research of the earthquakes induced by water injections in salt mines in Changning, Sichuan. Earthquake Research in China, 24(3), 226–234.

Schultz, R., Atkinson, G., Eaton, D. W., Gu, Y. J., & Kao, H. (2018). Hydraulic fracturing volume is associated with induced earthquake productivity in the Duvernay play. Science, 359(6373), 304-308. https://doi.org/10.1126/science.aao0159

Sun, B. (2018). Characteristics of structural deformation and fluid activity in Changning area and its' perphery, southern Sichuan. (Master's thesis) (in Chinese). Retrieved from CNKI. (http://www.cnki.net/). Chengdu: Chengdu University of Technology.

The six unit of the first district survey team of the Sichuan Provincial Geological Bureau (1973). The geological report of the Junlian region. Retrieved from: http://www.ngac.org.cn/Document/Document.aspx?MetaId=04F475FDB61D3C88E05341015A0AF7CD&DocId=440DF4784E4D26AFE05341015A0A5A98, (in Chinese), Accessed date: October 2019.

Yang, T., Fang, L. H., Wu, J. P., Wang, W. L, Lu, R. Q., Cheng, J., Han, L. B. & Fan, L. P. (2020). Aftershock sequence relocation of the Sichuan Changning M6.0 earthquake and its seismogenic structure, Tectonophysics (under review).

Yi, G. X., Long, F., Liang, M. J., Zhao, M., Wang, S. W., Gong, Y., Qiao, H. Z., & Su, J. R. (2019). Focal mechanism solutions and seisogenic structure of the 17 June 2019 Ms6.0 Sichuan Changning earthquake sequence. Chinese Journal Geophysics, 62(9): 3432-3447. https://doi.org/10.6038/cjg2019N0297

THANK YOU FOR WATCH

DESIGNED BY GAOHUA

E-mail: gaohuastudent@163.com